Bioorganic & Medicinal Chemistry Letters xxx (xxxx) xxx–xxx

Contents lists available at ScienceDirect

Bioorganic & Medicinal Chemistry Letters

journal homepage: www.elsevier.com/locate/bmcl

Radiosynthesis, biological evaluation and preliminary microPET study of ^{18}F-labeled 5-resorcinolic triazolone derivative based on ganetespib targeting HSP90

Julie Kang[a,1], Jun Young Lee[b,1], İsa Taş[a], Kunal N. More[a], Hangun Kim[a], Jeong-Hoon Park[b,*], Dong-Jo Chang[a,*]

[a] College of Pharmacy and Research Institute of Life and Pharmaceutical Sciences, Sunchon National University, Suncheon 57922,Republic of Korea
[b] Radiation Instrumentation Research Division, Korea Atomic Energy Research Institute, Jeongeup 56212, Republic of Korea

ARTICLE INFO

Keywords:
HSP 90
Tumor hypoxia
PET imaging
Ganetespib
TNBC breast cancer

ABSTRACT

Heat-shock protein 90 (HSP90) is a molecular chaperone that activates oncogenic transformation in several solid tumors, including lung and breast cancers. Ganetespib, a most promising candidate among several HSP90 inhibitors under clinical trials, has entered Phase III clinical trials for cancer therapy. Despite numerous evidences validating HSP90 as a target of anticancer, there are few studies on PET agents targeting oncogenic HSP90. In this study, we synthesized and biologically evaluated a novel ^{18}F-labeled 5-resorcinolic triazolone derivative (**1**, [^{18}F]PTP-Ganetespib) based on ganetespib. [^{18}F]PTP-Ganetespib was labeled by click chemistry of Ganetespib-PEG-Alkyne (**10**) and [^{18}F]PEG-N_3 (**11**) with 37.3 ± 5.11% of radiochemical yield and 99.7 ± 0.09% of radiochemical purity. [^{18}F]PTP-Ganetespib showed proper LogP (0.96 ± 0.06) and good stability in human serum over 97% for 2 h. [^{18}F]PTP-Ganetespib showed high uptakes in breast cancer cells containing triple negative breast cancer (TNBC) MDA-MB-231 and Her2-negative MCF-7 cells, which are target breast cancer cell lines of HSP90 inhibitor, ganetespib, as an anticancer. Blocking of HSP90 by the pretreatment of ganetespib exhibited significantly decreased accumulation of [^{18}F]PTP-Ganetespib in MDA-MB-231 and MCF-7 cells, indicating the specific binding of [^{18}F]PTP-Ganetespib to MDA-MB-231 and MCF-7 cells with high HSP90 expression. In the biodistribution and microPET imaging studies, the initial uptake into tumor was weaker than in other thoracic and abdominal organs, but [^{18}F]PTP-Ganetespib was retained relatively longer in the tumor than other organs. The uptake of [^{18}F]PTP-Ganetespib in tumors was not sufficient for further development as a tumor-specific PET imaging agent by itself, but this preliminary PET imaging study of [^{18}F]PTP-Ganetespib can be basis for developing new PET imaging agents based on HSP90 inhibitor, ganetespib.

Since the emergence of 2-deoxy-2-[^{18}F]fluoroglucose ([^{18}F]FDG) as a PET imaging agent for the diagnosis of cancer, a large number of PET imaging agents have been developed and entered in clinical trials. However, only a few PET imaging agents such as [^{11}C]choline and [^{18}F]fluciclovine have been used in clinics for imaging of cancer, and the number of clinically approved PET imaging agents for cancer is very limited as compared to the development of anticancer agents for therapy.[1] Currently, most PET tracers for imaging of cancer under preclinical and clinical trials are predominantly ligand-targeted imaging agents. Numerous targeted anticancer agents under clinical trials have been developed to target various classes of oncogenic proteins, including cell membrane receptors, nuclear membrane receptors, cytosolic proteins, cytoskeletons, and macromolecules in diverse organelles such as the mitochondria and ribosomes, as well as genetic entities in the nucleus such as histone and DNA.[2] On the other hand, most targeted imaging agents, including PET tracers, under preclinical and clinical trials have been developed to target oncogenic membrane receptors such as folate receptor (FR), prostate-specific membrane antigen (PSMA), $\alpha_v\beta_3$ integrin, somatostatin receptor 2 (SSTR2), and glucagon-like peptide 1 receptor (GLP1R).[3] As examples, [^{99m}Tc]etarfolatide,[4] [^{68}Ga]DOTANOC,[5,6] and [^{111}In]exendin-4,[7] currently developed in Phase III clinical trials target FR, SSTR2, and GLP1R, respectively. As a number of anticancer drugs targeting various classes of oncogenic proteins have been developed, cytoplasmic oncogenic

* Corresponding authors.
E-mail addresses: parkjh@kaeri.re.kr (J.-H. Park), djchang@sunchon.ac.kr (D.-J. Chang).
[1] The first two authors contributed equally to this work.

https://doi.org/10.1016/j.bmcl.2018.10.035
Received 16 August 2018; Received in revised form 21 October 2018; Accepted 22 October 2018

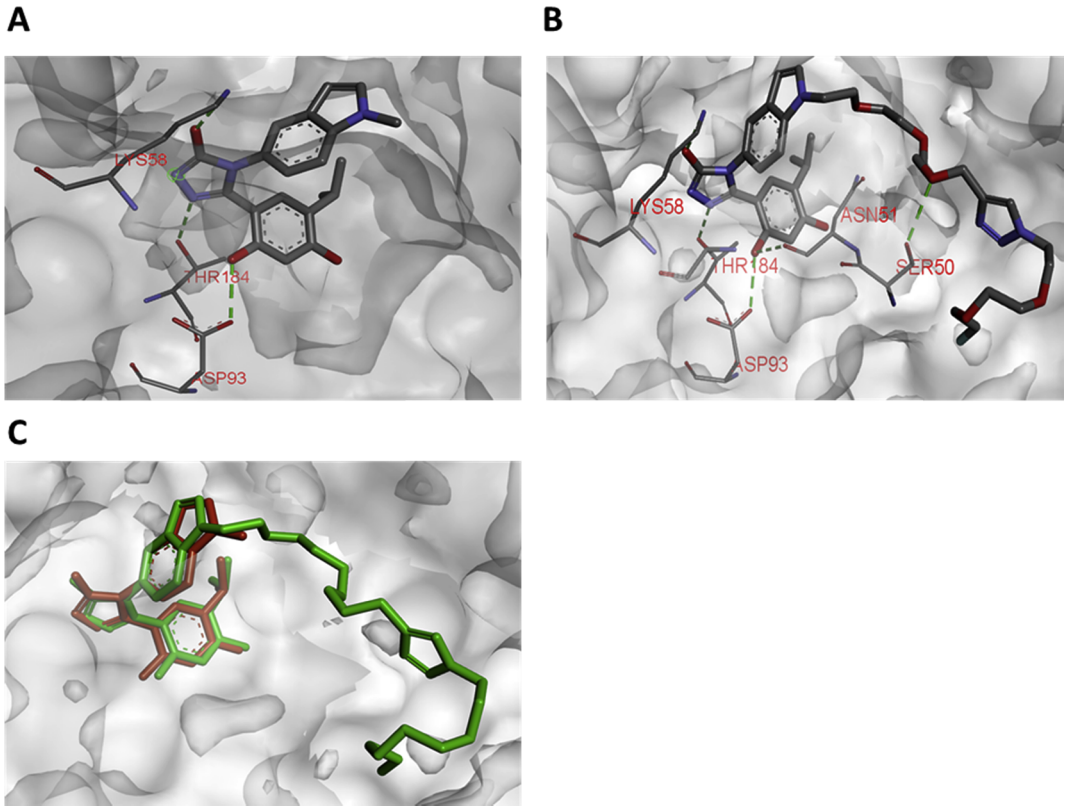

Fig. 1. A. Molecular docking in the *N*-terminal ATP binding pocket of human HSP90. A. X-ray co-crystal structure of ganetespib (H-bonds, green color); B. Molecular docking of [^{19}F]PTP-Ganetespib (H-bonds, green color); C. Superimposition of [^{19}F]PTP-Ganetespib (green color) with ganetespib (red color). (For interpretation of the references to color in this figure legend, the reader is referred to the web version of this article.)

proteins such as HSP90 can be also potential targets for the development of clinically available PET imaging agents.

Heat-shock protein 90 (HSP90) is an ATP-dependent molecular chaperone that induces a conformational change of its client protein by associating with other co-chaperones.[8,9] HSP90 regulates various oncogenic processes, including apoptosis, angiogenesis, invasion, and tumor growth, stabilizes and activates several oncogenic client proteins such as HIF-1α, Akt, Her2, and EGFR, which are involved in various signal transduction pathways in cancer.[10–13] HSP90 is a constitutively expressed chaperone in most cells of normal tissues and it accounts for 1–2% of all cellular proteins. However, specific stimuli such as phosphorylation, ligand binding, dimerization, oxidative stress and hypoxia result in an approximately two-fold increase of HSP90 levels, which has been found to be essential for oncogenic transformation.[12,14] Since the discovery of geldanamycin as an HSP90 inhibitor, several HSP90 inhibitors have been developed and entered in clinical trials.[15–17] Early HSP90 inhibitors, including the ansanamycin-based compounds such as 17-allylamino-17-demethoxy geldanamycin (17-AAG)[18,19] and 17-dimethylamino ethylamino-17-demethoxygeldanamycin (17-DMAG),[20] and the purine-based compounds such as CNF2024/BIIB021[21,22] and MPC-0767,[23] have shown promising anticancer activity. However, they were not considered for further development due to their poor pharmacokinetic properties and mechanism-based side effects such as hepatic toxicity.[24] Based on the evidence from the clinical trials on geldanamycin derivatives, several synthetic HSP90 inhibitors with novel scaffolds such as pyrazole (CCT018159 and VER-49009) and isoxazole (NVP-AUY922) have been discovered from chemical libraries and structure-based drug designs,[25–27] and have subsequently entered in clinical trials.[28] Of various HSP90 inhibitors, NVP-AUY922 and NVP-HSP990 developed by Novartis have shown good efficacy and acceptable safety profiles in Phase I/II clinical trials.[29,30] Quite recently, Synta Pharmaceutical Corp. has discovered another class of HSP90 inhibitor with a triazole scaffold called STA-9090 (Ganetespib).[31–34] Gantespib exhibits a high affinity to HSP90, and shows promising anticancer activity against solid tumors and hematological malignancies. Ganetespib has not shown hepatotoxicity that was observed in the early HSP90 inhibitors such as the geldanamycin derivatives.[24,35,36] Ganetespib with a 5-resorcinolic triazolone scaffold has a high affinity for HSP90 (IC_{50} ~ 10 nM) and has shown higher uptake into tumors than other organs in clinical trials as well as *in vivo* models,[24,34,37,38] suggesting ganetespib can be a potential ligand for the development of PET imaging agent for cancer and also HSP90 can be a potential target for imaging of cancer as well as cancer therapy.[24,39] However, there are only a limited number of studies on the development of imaging agents targeting HSP90, including PET radiotracers. To date, only one study has been reported for the development of PET imaging agents targeting HSP90 using the early HSP90 inhibitor, PU-H71, that targets Her2-positive breast cancer and triple negative breast cancer.[40]

In this study, we synthesized ^{18}F-labeled tracer (**1**, [^{18}F]PTP-Ganetespib) based on an HSP90 inhibitor, ganetespib, and performed a preliminary PET study in order to develop a new PET imaging agent for cancer and validate cytoplasmic HSP90, not a membrane receptor, as a potential target for imaging of cancer. We chose ganetespib as a ligand targeting HSP90 because it is one of the most promising candidates in current clinical trials for the development of anticancer agents targeting HSP90.

Ying reported the X-ray co-crystal structure of ganetespib bound to the *N*-terminal ATP-binding pocket of HSP90, which revealed that 5-resorcinolic triazolone group of ganetespib makes two hydrogen bondings with Asp93 and Lys58 in the active site of HSP90, while the indole group is aligned towards the outside.[41] Based on the analysis of X-ray co-crystal structure of ganetespib, we designed a [^{18}F]PTP-Ganetespib (**1**) with a ^{18}F-labeled PEG linker at indole group. Considering the efficient synthesis, we planned to introduce [^{18}F] by the click

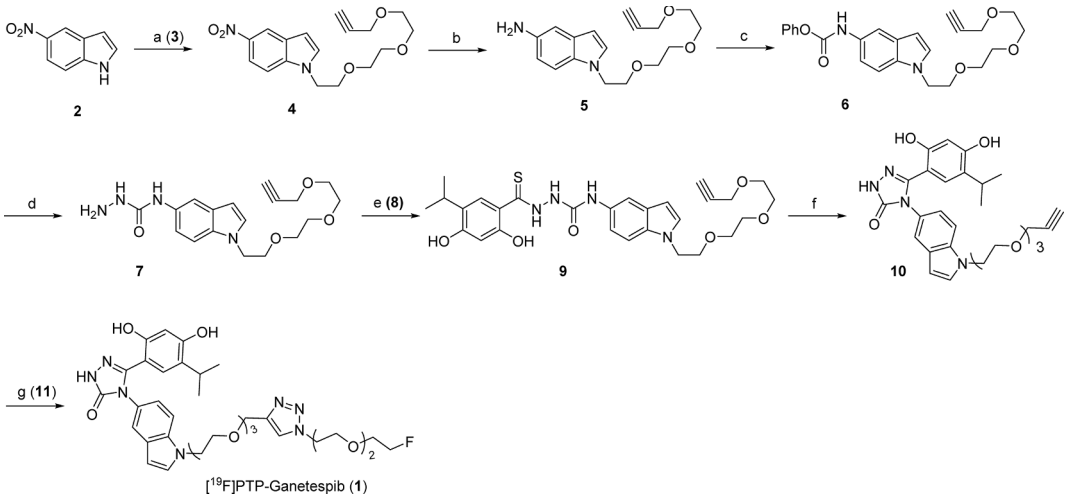

Scheme 1. Reagents and conditions for synthesis of cold [^{19}F]PTP-Ganetespib (**1**): (a) NaH, 2-(2-(2-(prop-2-yn-1-yloxy)ethoxy)ethoxy)ethyl 4-methylbenzenesulfonate (**3**), DMF, 99%; (b) $SnCl_2{\cdot}H_2O$, EtOH, reflux, 80%; (c) Phenyl chloroformate, Et_3N, CH_2Cl_2, 0 °C, 83%; (d) Hydrazine monohydrate, dioxane, *mw*, 88%; (e) Chloroacetic acid, $NaHCO_3$, 2,4-dihydroxy-5-isopropylbenzodithioic acid (**8**), DMF, 68%; (f) KOH, MeOH, 75 °C, 27%; (g) $CuSO_4{\cdot}5H_2O$, sodium ascorbate, [^{19}F]PEG-N_3 (**11**), 60%.

reaction of ganetespib bearing a PEG-alkyne group (Ganetespib-PEG-Alkyne) with a ^{18}F-labeled PEG linker bearing an azide ([^{18}F]PEG-N_3).[42] Prior to the synthesis and evaluation of [^{18}F]PTP-Ganetespib, a molecular docking study using the crystal structure of human HSP90 complexed with ganetespib (PDB:3TUH)[41] was carried out to investigate whether tracer **1** with a triazole-PEG linker can bind to HSP90 compared to its parent ligand, ganetespib. The molecular docking revealed that [^{18}F]PTP-Ganetespib (**1**) rests very well in the *N*-terminal ATP binding pocket of HSP90 and the binding mode of 5-resorcinolic triazolone moiety in tracer **1** is the almost same as ganetespib. A hydroxyl group of resorcinol and a carbonyl group of triazolone make two H-bondings with Asp93 and Lys58, respectively, and the N^2 atom of triazolone facilitates H-bonding with Thr184, similar to ganetespib (Fig. 1B). Fluorinated PEG linker of tracer **1** protrudes from the pocket and interacts well in the outside of the ATP-binding pocket. The superimposition of ganetespib with tracer **1** showed that they have the almost same conformation and alignment in the ATP-binding pocket (Fig. 1C).

Scheme 1 illustrates the synthesis of cold [^{19}F]PTP-Ganetespib (**1**). Alkylation of 5-nitroindole with alkyne-PEG-sulfonate (**3**) followed by reduction using $SnCl_2{\cdot}H_2O$ produced the intermediate **5**. The formylation of **5** with phenyl chloroformate and the subsequent substitution reaction with hydrazine afforded the hydrazide **7**.[43] The precursor **10** of click reaction with a triazolone group was synthesized by the coupling reaction of the hydrazide **7** with benzodithioic acid (**8**)[43,44] and the subsequent intramolecular cyclization using potassium hydroxide in methanol.[45] The synthesis of cold [^{19}F]PTP-Ganetespib was completed by the click reaction of Ganetespib-PEG-Alkyne (**10**) with [^{19}F]PEG-N_3 (**11**) in the presence of $CuSO_4{\cdot}5H_2O$ and sodium ascorbate. ^{18}F-Radiolabeling of the tosylated PEG linker bearing an azide group (**12**, N_3-PEG-OTs) with [2,2,2]-cryptand in acetonitrile successfully provided a ^{18}F-labeled PEG linker with an azide group (**11**, [^{18}F]PEG-N_3) with 57.5 ± 5.95% (n = 4) of radiochemical yield and 99.3 ± 0.03% (n = 3) of radiochemical purity. Finally, [^{18}F]PTP-Ganetespib (**1**) was produced by the click reaction of the precursor **10** with [^{18}F]PEG-N_3 (**11**) in the same condition as synthesis of [^{19}F]PTP-Ganetespib (Scheme 2). It resulted in 37.3 ± 5.11% (n = 4) of radiochemical yield, 99.7 ± 0.09% (n = 3) of radiochemical purity, and 1.70 GBq/μmol of the specific activity after the purification by reverse phase HPLC (Fig. 2).

As presented in Fig. 3, the physicochemical properties of [^{18}F]PTP-Ganetespib were evaluated by measuring hydrophobicity and stability in human serum. [^{18}F]PTP-Ganetespib exhibited 0.96 ± 0.06 of LogP (ESI†, Table S1), which suggests tracer **1** probably has a suitable cell permeability and *in vivo* distribution as an imaging agent targeting an intracellular protein. In the stability test, [^{18}F]PTP-Ganetespib

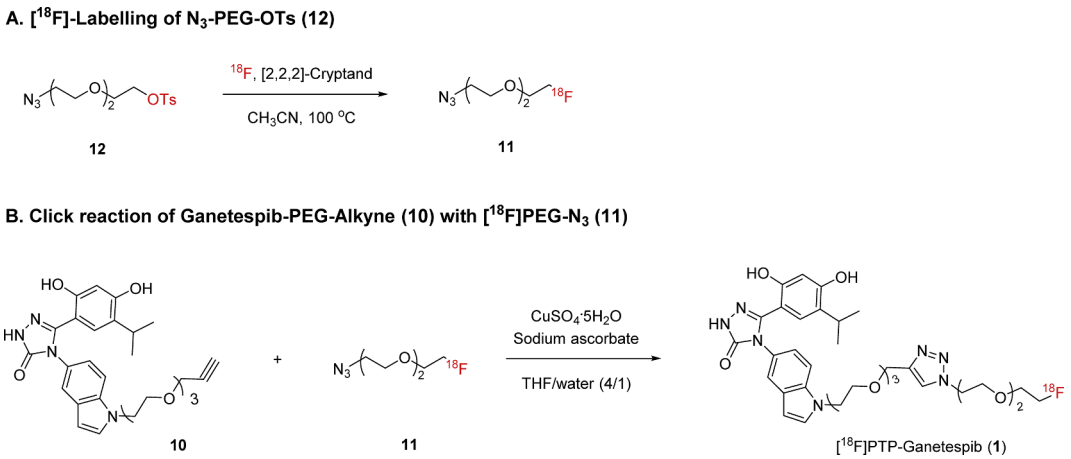

Scheme 2. Reagents and conditions for radiosynthesis of [^{18}F]PTP-Ganetespib (**1**): A. ^{18}F-Labeling of N_3-PEG-OTs (**12**); B. Click reaction of Ganetespib-PEG-Alkyne (**10**) with [^{18}F]PEG-N_3 (**11**).

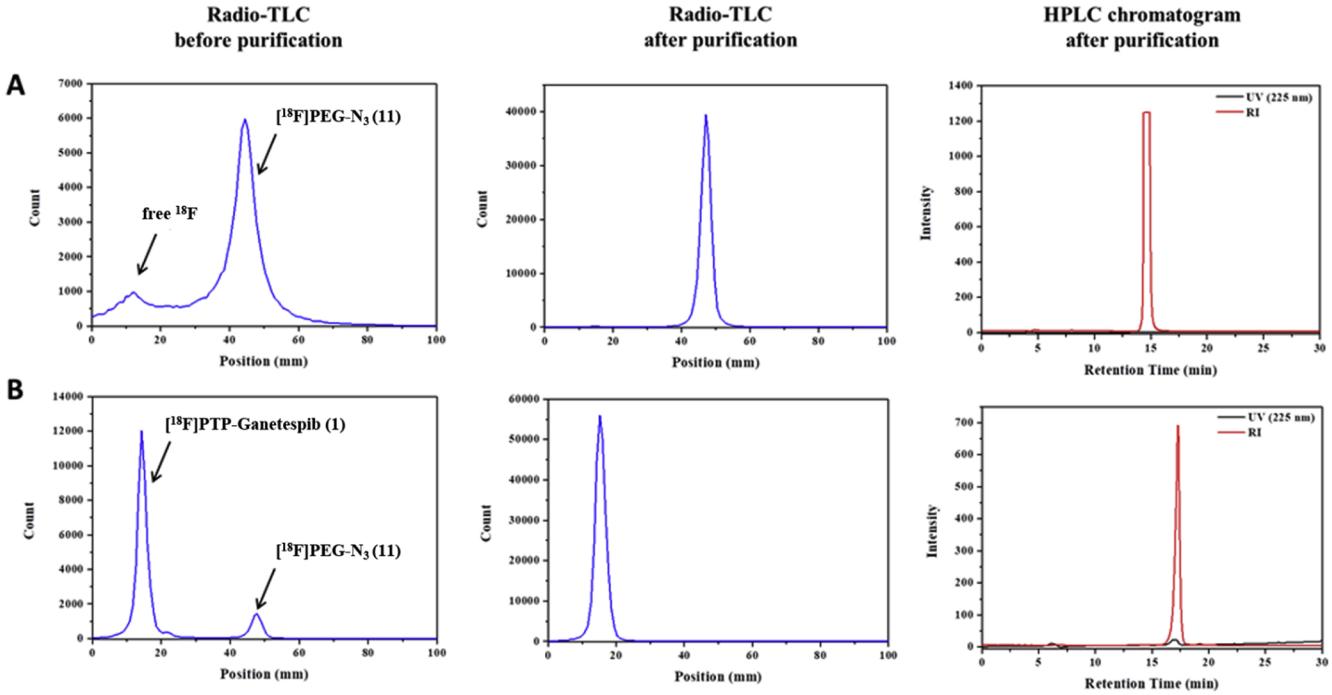

Fig. 2. Analysis of ^{18}F-labeled precursor of click reaction and [^{18}F]PTP-Ganetespib (**1**). A. Radio-TLC and HPLC chromatogram of [^{18}F]PEG-N_3 (**11**) after HPLC purification, B. Radio-TLC and HPLC chromatogram of [^{18}F]PTP-Ganetespib (**1**).

exhibited a high stability in human serum up to 2 h post-labeling and purification by HPLC. [^{18}F]PTP-Ganetespib (**1**) showed the retained radiochemical purity over 97% in triplicate tests (Fig. 3).

Clinical trials of ganetespib in combination therapies with cytotoxic agents as well as a single anticancer agent have been conducted against several solid tumors, including non-small cell lung cancer (NSCLC) and breast cancer.[14] Also, ganetespib has shown potent anticancer effect in preclinical studies using *in vitro* and *in vivo* breast cancer models.[46,47] Preclinical studies showed that ganetespib has a strong anticancer effect on a broad spectrum of breast cancer subtypes, including triple negative breast cancer (TNBC) and Her2-negative breast cancer such as MDA-MB-231 and MCF-7 cells, respectively.[46] Based on reported preclinical studies of ganetespib, we carried out cell uptake test of [^{18}F]PTP-Ganetespib in MDA-MB-231 cells and MCF-7 cells. The accumulation of [^{18}F]PTP-Ganetespib increased linearly with time in both MDA-MB-231 and MCF-7 cells and showed a specific accumulation of 3.30 ± 0.05 ID % and 2.99 ± 0.28 ID%, respectively, at the final time interval of

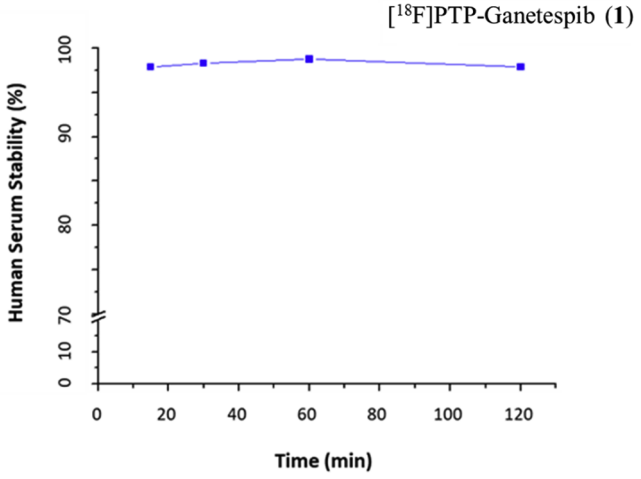

Fig. 3. A. Stability of [^{18}F]PTP-Ganetespib (**1**) in human serum.

120 min (Fig. 4A and Table S3 in ESI†). Furthermore, we confirmed specific uptake of [^{18}F]PTP-Ganetespib into MDA-MB-231 and MCF-7 cells by blocking of HSP90 using the pretreatment of ganetespib. To confirm the uptake capacity of [^{18}F]PTP-Ganetespib to HSP90 in these two cells, we incubated MDA-MB-231 and MCF-7 cells with 50 μg of ganetespib and then treated [^{18}F]PTP-Ganetespib (Fig. 4B and 4C, Table S4 in ESI†). In competitive assay, the uptake of [^{18}F]PTP-Ganetespib was dramatically inhibited by the pretreated ganetespib in both cell lines. Cellular uptake of [^{18}F]PTP-Ganetespib was decreased to below 1 ID% at the final time interval of 120 min by blocking HSP90 with ganetespib. This result clearly implies that our tracer can specifically bind to MDA-MB-231 and MCF-7 cells with high HSP90 expression although we did not determine the binding affinity of radiotracer **1**.

Based on the result of cellular uptake study, the biodistribution of [^{18}F]PTP-Ganetespib was evaluated on orthotopic breast cancer xenografts with MDA-MD-231 tumors. [^{18}F]PTP-Ganetespib was administered to xenografts by intravenous injection (3.7 MBq), followed by detection of uptake signals at the time intervals of 15, 60, and 120 min post-injection (p.i). The biodistribution data of tracer **1** for tumors, blood, muscle, and other peripheral organs such as heart, lung, liver, spleen, stomach, intestine, pancreas, kidney, tail, skin, and brain is listed in Fig. 5A. Initially, the abdominal and thoracic regions, including intestine, stomach, kidney, liver, and lung, showed much higher uptake than tumors at 15 min p.i. [^{18}F]PTP-Ganetespib was rapidly eliminated from kidney over time, and showed relatively slow clearance in liver. However, most organs exhibited a linear decrease in signal intensity with time, whereas the radioactivity in tumors was relatively less decreased or maintained up to 120 min p.i. At the final interval of 120 min p.i, more than 1 %ID/g of radioactivity was observed in the liver, stomach, intestine, bone, skin, and tumors, whereas the blood, heart, spleen, pancreas, kidney, muscle, and brain showed faster elimination than tumors. [^{18}F]PTP-Ganetespib showed 1.13 %ID/g of uptake in tumors at 60 min p.i, which was retained by 1.08 ± 0.16 at 120 min p.i. The ratios of tumor to blood (T/B) and tumor to muscle (T/M) increased with time, and reached to 1.31 ± 0.34 and 1.78 ± 0.53, respectively, at 120 min p.i., which was correlated with *in vitro* cellular uptake. As shown in time-activity curves (TACs) based on

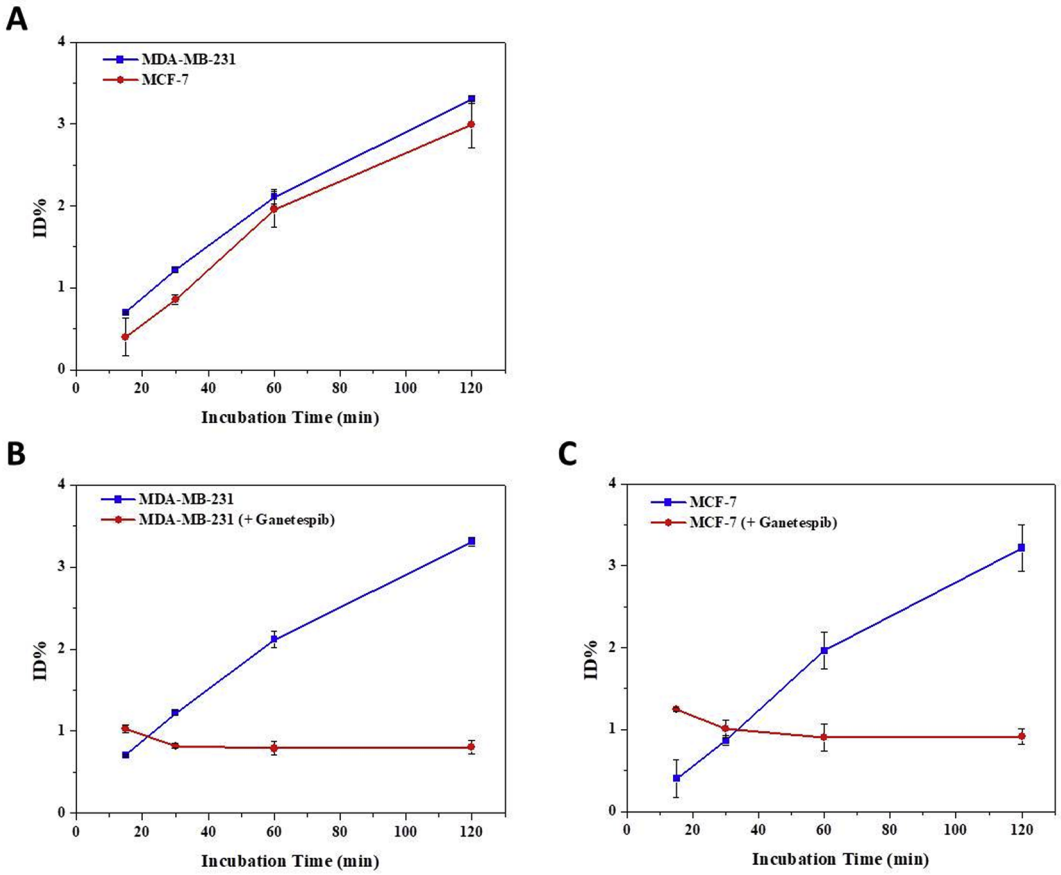

Fig. 4. A. Cell uptake of [^{18}F]PTP-Ganetespib (**1**) in MDA-MB-231 and MCF-7 cells, B. Cell uptake of [^{18}F]PTP-Ganetespib (**1**) in MDA-MB-231 cells with blocking of HSP90 by the pretreatment of ganetespib, C. Cell uptake of [^{18}F]PTP-Ganetespib (**1**) in MCF-7 cells with blocking of HSP90 by the pretreatment of ganetespib.

ex vivo biodistribution study (Fig. 5B), [^{18}F]PTP-Ganetespib showed a high distribution of 1.45 ± 0.40 %ID/g up to 60 min in static flow of blood and then was slowly decreased, whereas the distribution into the tumor was slightly increased or maintained up to the final time interval of 120 min. However, [^{18}F]PTP-Ganetespib does not show enough tumor-specific distribution for PET imaging although giving promising results *in vitro*. The accumulation of tracer **1** tends to increase only in the bones and tumors. The absorption of free ^{18}F into bones was widely reported in many previous studies[48,49], but in our case, the tracer **1** showed very low uptake into bones (< 1% ID/g, ESI†, Table S5).

MicroPET study was performed to evaluate the distribution of [^{18}F]PTP-Ganetespib in the animal's whole body, and to investigate tumor-specific uptake in orthotopic TNBC xenografts bearing MDA-MB-231 tumors (Fig. 6). The imaging was carried out at the intervals of 15, 60 and 120 min p.i. At the first interval of 15 min p.i, a high uptake was mainly detected in the thoracic and abdominal regions such as the lung, liver, intestine, and kidney. The signal from tumors was also detected but it was relatively weak as compared to the background tissues.

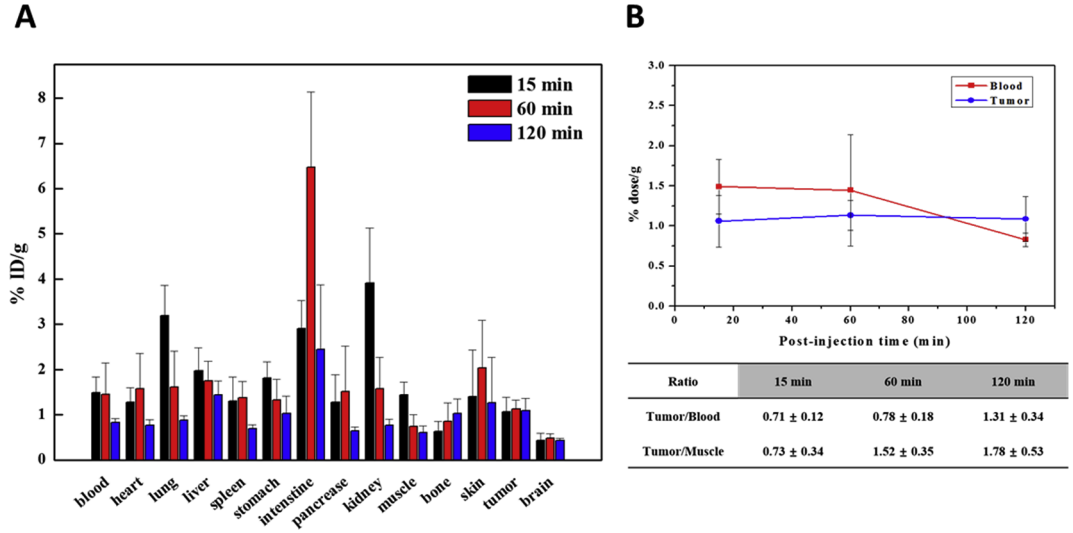

Ratio	15 min	60 min	120 min
Tumor/Blood	0.71 ± 0.12	0.78 ± 0.18	1.31 ± 0.34
Tumor/Muscle	0.73 ± 0.34	1.52 ± 0.35	1.78 ± 0.53

Fig. 5. Biodistribution of [^{18}F]PTP-Ganetespib (**1**) on orthotopic TNBC xenograft mice bearing MDA-MB-231 tumors at 15, 60 and 120 min post injection.

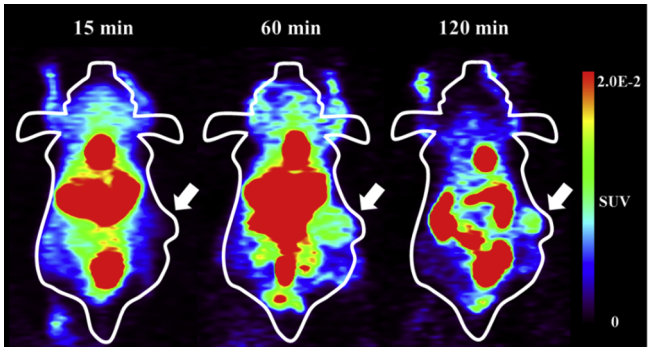

Fig. 6. MicroPET images of [^{18}F]PTP-Ganetespib (**1**) in orthotopic TNBC xenografts bearing MDA-MB-231 tumors at 15, 60 and 120 min post injection. The white arrows indicate the tumors.

However, although weaker than the signals from the thoracic and abdominal regions, the uptake signals in tumor relatively increased with time as compared to the signals from other organs. These PET images showed that [^{18}F]PTP-Ganetespib is retained longer and excreted more slowly in tumor than thoracic and abdominal regions although showing very low accumulation into tumor, which is entirely consistent with the result of biodistribution study. These *in vivo* studies of [^{18}F]PTP-Ganetespib, including biodistribution and PET imaging, suggest that radiotracer **1** can provide a basis for the discovery of a PET tracer targeting HSP90, which can be achieved by the structural modification such as changing the length or type of the linker connecting the radioactive functional group (^{18}F) to targeting ligand, ganetespib.

In conclusion, we designed a ^{18}F-labeled 5-resorcinolic triazolone derivative based on ganetespib targeting HSP90 by molecular modeling, and successfully synthesized [^{18}F]PTP-Ganetespib (**1**) by the click chemistry of alkyne (Ganetespib-PEG-Alkyne) with ^{18}F-labeled azide ([^{18}F]PEG-N_3). [^{18}F]PTP-Ganetespib showed good stability in human serum, adequate hydrophobicity for permeation, and high *in vitro* cell uptake in TNBC MDA-MB-231 and Her2-negative MCF-7 cells. Specific binding of [^{18}F]PTP-Ganetespib to two cell lines with HSP90 was confirmed by blocking test using ganetespib. The biodistribution and microPET imaging of [^{18}F]PTP-Ganetespib were evaluated in orthotopic TNBC xenograft models with MDA-MB-231 tumors. This is the first PET imaging study using a recent HSP90 inhibitor with a triazolone scaffold which has been currently developed in clinical trials. Although [^{18}F]PTP-Ganetespib did not show enough accumulation in tumor *in vivo* and would be considered a poor candidate for HSP90 imaging, it showed relatively slower excretion from tumor as compared to other organs in orthotopic TNBC xenografts.

Acknowledgments

This work was supported by the National Research Foundation of Korea (NRF) funded by the Ministry of Science, ICT & Future Planning (NRF-2016R1C1B1009901, 2016M2B2A4909218 and 2017M2A2A6A05016600).

Appendix A. Supplementary data

Supplementary data to this article can be found online at https://doi.org/10.1016/j.bmcl.2018.10.035.

References

1. Opacic T, Paefgen V, Lammers T, Kiessling F. Status and trends in the development of clinical diagnostic agents. *Wiley Interdiscip Rev: Nanomed Nanobiotechnol.* 2017;9(4).
2. Santos R, Ursu O, Gaulton A, et al. A comprehensive map of molecular drug targets. *Nat Rev Drug Discovery.* 2017;16(1):19–34.
3. Srinivasarao M, Galliford CV, Low PS. Principles in the design of ligand-targeted cancer therapeutics and imaging agents. *Nat Rev Drug discovery.* 2015;14(3):203–219.
4. Palmer E, Scott J, Symanowski J. Reliability and reproducibility of etarfolatide as a folate receptor (FR)-targeted diagnostic imaging agent. *J Nucl Med.* 2013;54(supplement 2):400.
5. Klinaki I, Al-Nahhas A, Soneji N, Win Z. 68Ga DOTATATE PET/CT uptake in spinal lesions and MRI correlation on a patient with neuroendocrine tumor: potential pitfalls. *Clin Nucl Med.* 2013;38(12):449–453.
6. Haug AR, Cindea-Drimus R, Auernhammer CJ, et al. Neuroendocrine tumor recurrence: diagnosis with 68Ga-DOTATATE PET/CT. *Radiology.* 2014;270(2):517–525.
7. Christ E, Wild D, Reubi JC. Glucagonlike peptide-1 receptor: an example of translational research in insulinomas: a review. *Endocrinol Metab Clin North Am.* 2010;39(4):791–800.
8. Neckers L. Heat shock protein 90: the cancer chaperone. *J Biosci.* 2007;32(3):517–530.
9. Trepel J, Mollapour M, Giaccone G, Neckers L. Targeting the dynamic HSP90 complex in cancer. *Nat Rev Cancer.* 2010;10(8):537–549.
10. Bagatell R, Whitesell L. Altered Hsp90 function in cancer: a unique therapeutic opportunity. *Mol Cancer Ther.* 2004;3(8):1021–1030.
11. Sõti C, Nagy E, Giricz Z, Vígh L, Csermely P, Ferdinandy P. Heat shock proteins as emerging therapeutic targets. *Br J Pharmacol.* 2005;146(6):769–780.
12. Whitesell L, Lindquist SL. HSP90 and the chaperoning of cancer. *Nat Rev Cancer.* 2004;5(10):761–772.
13. Schopf FH, Biebl MM, Buchner J. The HSP90 chaperone machinery. *Nat Rev Mol Cell Biol.* 2017;18(6):345–360.
14. Buchner J. Hsp90 & Co.–a holding for folding. *Trends Biochem Sci.* 1999;24(4):136–141.
15. Sidera K, Patsavoudi E. HSP90 inhibitors: current development and potential in cancer therapy. *Recent Pat Anticancer Drug Discov.* 2014;9(1):1–20.
16. Khandelwal A, Crowley VM, Blagg BS. Natural product inspired N-terminal Hsp90 inhibitors: from bench to bedside? *Med Res Rev.* 2016;36(1):92–118.
17. Gewirth DT. Paralog specific Hsp90 Inhibitors–a brief history and a bright future. *Curr Top Med Chem.* 2016;16(25):2779–2791.
18. Whitesell L, Mimnaugh EG, De Costa B, Myers CE, Neckers LM. Inhibition of heat shock protein HSP90-pp60v-src heteroprotein complex formation by benzoquinone ansamycins: essential role for stress proteins in oncogenic transformation. *Proc Natl Acad Sci USA.* 1994;91(18):8324–8328.
19. Neckers L, Schulte TW, Mimnaugh E. Geldanamycin as a potential anti-cancer agent: its molecular target and biochemical activity. *Invest New Drugs.* 1999;17(4):361–373.
20. Schulte TW, Neckers LM. The benzoquinone ansamycin 17-allylamino-17-demethoxygeldanamycin binds to HSP90 and shares important biologic activities with geldanamycin. *Cancer Chemother Pharmacol.* 1998;42(4):273–279.
21. Zhang H, Neely L, Lundgren K, et al. BIIB021, a synthetic Hsp90 inhibitor, has broad application against tumors with acquired multidrug resistance. *Int J Cancer.* 2010;126(5):1226–1234.
22. Lundgren K, Zhang H, Brekken J, et al. BIIB021, an orally available, fully synthetic small-molecule inhibitor of the heat shock protein Hsp90. *Mol Cancer Ther.* 2009;8(4):921–929.
23. Bajji AC, Kim S-H, Markovitz B, et al. Therapeutic compounds and their use in cancer. WO2007134298.
24. Jhaveri K, Modi S. Ganetespib: research and clinical development. *OncoTargets Ther.* 2015;8:1849–1858.
25. Cheung K-MJ, Matthews TP, James K, et al. The identification, synthesis, protein crystal structure and in vitro biochemical evaluation of a new 3, 4-diarylpyrazole class of Hsp90 inhibitors. *Bioorg Med Chem Lett.* 2005;15(14):3338–3343.
26. Sharp SY, Boxall K, Rowlands M, et al. In vitro biological characterization of a novel, synthetic diaryl pyrazole resorcinol class of heat shock protein 90 inhibitors. *Cancer Res.* 2007;67(5):2206–2216.
27. Eccles SA, Massey A, Raynaud FI, et al. NVP-AUY922: a novel heat shock protein 90 inhibitor active against xenograft tumor growth, angiogenesis, and metastasis. *Cancer Res.* 2008;68(8):2850–2860.
28. Tatokoro M, Koga F, Yoshida S, Kihara K. Heat shock protein 90 targeting therapy: state of the art and future perspective. *EXCLI J.* 2015;14:48–58.
29. Menezes DL, Taverna P, Jensen MR, et al. The novel oral Hsp90 inhibitor NVP-HSP990 exhibits potent and broad-spectrum antitumor activities in vitro and in vivo. *Mol Cancer Ther.* 2012;11(3):730–739.
30. Lamottke B, Kaiser M, Mieth M, et al. The novel, orally bioavailable HSP90 inhibitor NVP-HSP990 induces cell cycle arrest and apoptosis in multiple myeloma cells and acts synergistically with melphalan by increased cleavage of caspases. *Eur J Haematol.* 2012;88(5):406–415.
31. Ying W, Sun L, Koya K, et al. Triazole compounds that modulate Hsp90 activity. WO2009023211.
32. Ying W, Foley K. Triazole derivatives as HSP90 modulators. WO2008021364.
33. Chimmanamada D, Burlison J, Ying W, et al. Triazole compounds that are useful in the treatment of proliferative disorders, such as cancer. WO2008097640.
34. Lin T-Y, Bear M, Du Z, et al. The novel HSP90 inhibitor STA-9090 exhibits activity against Kit-dependent and-independent malignant mast cell tumors. *Exp Hematol.* 2008;36(10):1266–1277.
35. He S, Smith DL, Sequeira M, Sang J, Bates RC, Proia DA. The HSP90 inhibitor ganetespib has chemosensitizer and radiosensitizer activity in colorectal cancer. *Invest New Drugs.* 2014;32(4):577–586.
36. Ying W, Du Z, Sun L, et al. Ganetespib, a unique triazolone-containing Hsp90 inhibitor, exhibits potent antitumor activity and a superior safety profile for cancer therapy. *Mol Cancer Ther.* 2012;11(2):475–484.
37. Shimamura T, Perera SA, Foley KP, et al. Ganetespib (STA-9090), a nongeldanamycin HSP90 inhibitor, has potent antitumor activity in in vitro and in vivo models of non–small cell lung cancer. *Clin Cancer Res.* 2012;18(18):4973–4985.
38. Ying W, Chimmanamada D, Zhang J, et al. Hsp90 inhibitor drug conjugates (HDCs):

Construct design and preliminary evaluation. *AACR.* 2014.
39. Jhaveri K, Taldone T, Modi S, Chiosis G. Advances in the clinical development of heat shock protein 90 (Hsp90) inhibitors in cancers. *Biochim Biophys Acta.* 2012;1823(3):742–755.
40. Gerecitano JF, Modi S, Gajria D, et al. Using 124I-PU-H71 PET imaging to predict intratumoral concentration in patients on a phase I trial of PU-H71. *ASCO.* 2013.
41. Ying W. Crystal Structure of the N-terminal domain of an HSP90 in the presence of an the inhibitor ganetespib: http://www.rcsb.org/structure/3TUH.
42. Cao J, Liu Y, Zhang L, et al. Synthesis of novel PEG-modified nitroimidazole derivatives via "hot-click" reaction and their biological evaluation as potential PET imaging agent for tumors. *J Radioanal Nucl Chem.* 2017;312(2):263–276.
43. Chimmanamada DU, Zhang S, Lee C-W, Przewloka T, Ying W. Method for synthesis of triazole compounds that modulate hsp90 activity. WO2009075890.
44. Brough PA, Aherne W, Barril X, et al. 4, 5-diarylisoxazole Hsp90 chaperone inhibitors: potential therapeutic agents for the treatment of cancer. *J Med Chem.* 2007;51(2):196–218.
45. Bravo Y, Baccei CS, Broadhead A, et al. Identification of the first potent, selective and bioavailable PPARα antagonist. *Bioorg Med Chem Lett.* 2014;24(10):2267–2272.
46. Friedland JC, Smith DL, Sang J, et al. Targeted inhibition of Hsp90 by ganetespib is effective across a broad spectrum of breast cancer subtypes. *Invest New Drugs.* 2014;32(1):14–24.
47. Proia DA, Zhang C, Sequeira M, et al. Preclinical activity profile and therapeutic efficacy of the HSP90 inhibitor ganetespib in triple-negative breast cancer. *Clin Cancer Res.* 2014;20(2):413–424.
48. Lundblad H, Karlsson-Thur C, Maguire GQ, et al. Can spatiotemporal fluoride (18 F−) uptake be used to assess bone formation in the Tibia? a longitudinal study using PET/CT. *Clin Orthop Relat Res.* 2017;475(5):1486–1498.
49. Czernin J, Satyamurthy N, Schiepers C. Molecular mechanisms of bone 18F-NaF deposition. *J Nucl Med.* 2010;51(12):1826–1829.